Geotechnical and performance assessment impacts of DPC disposal in various host rock environments

Spent Fuel and Waste Disposition

Prepared for
U.S. Department of Energy
Spent Fuel and Waste Science and Technology
Jonny Rutqvist

Lawrence Berkeley National Laboratory

June 21, 2019
LBNL-2001220
SFWD Working Document: External Release

This page is intentionally left blank.

Revision 0
02/14/2019

APPENDIX E

NTRD DOCUMENT COVER SHEET [1]

Name/Title of Deliverable/Milestone/Revision No.	Geotechnical and performance assessment impacts of DPC disposal in various host rock environments/M4SF-19LB010305041
Work Package Title and Number	Direct Disposal of Dual Purpose Canisters - LBNL SF-19LB01030504
Work Package WBS Number	1.08.01.03.05
Responsible Work Package Manager	Jonny Rutqvist (signature on file) (Name/Signature)

Date Submitted **6/21/2019**

Quality Rigor Level for Deliverable/Milestone[2]	☐ QRL-1 Nuclear Data	☐ QRL-2	☐ QRL-3	☒ QRL 4 Lab-specific [3]

This deliverable was prepared in accordance with Lawrence Berkeley National Laboratory (LBNL)
(Participant/National Laboratory Name)

QA program which meets the requirements of
☒ DOE Order 414.1 ☐ NQA-1 ☐ Other

This Deliverable was subjected to:

☐ Technical Review
Technical Review (TR)
Review Documentation Provided
☐ Signed TR Report or,
☐ Signed TR Concurrence Sheet or,
☒ Signature of TR Reviewer(s) below
Name and Signature of Reviewers
Mengsu Hu
(Signature on file)
Boris Faybishenko: All Sections
(Signature on file)

☐ Peer Review
Peer Review (PR)
Review Documentation Provided
☐ Signed PR Report or,
☐ Signed PR Concurrence Sheet or,
☐ Signature of PR Reviewer(s) below
Name and Signature of Reviewers

NOTE 1: *Appendix E should be filled out and submitted with each deliverable. Or, if the PICS:NE system permits, completely enter all applicable information in the PICS:NE Deliverable Form. The requirement is to ensure that all applicable information is entered either in the PICS:NE system or by using the FCT Document Cover Sheet.*

- *In some cases there may be a milestone where an item is being fabricated, maintenance is being performed on a facility, or a document is being issued through a formal document control process where it specifically calls out a formal review of the document. In these cases, documentation (e.g., inspection report, maintenance request, work planning package documentation or the documented review of the issued document through the document control process) of the completion of the activity, along with the Document Cover Sheet, is sufficient to demonstrate achieving the milestone.*

NOTE 2: *If QRL 1, 2, or 3 is not assigned, then the QRL 4 box must be checked, and the work is understood to be performed using laboratory specific QA requirements. This includes any deliverable developed in conformance with the respective National Laboratory / Participant, DOE or NNSA-approved QA Program*

NOTE 3: *If the lab has an NQA-1 program and the work to be conducted requires an NQA-1 program, then the QRL-1 box must be checked in the work Package and on the Appendix E cover sheet and the work must be performed in accordance with the Lab's NQA-1 program. The QRL-4 box should not be checked*

This page intentionally left blank.

TABLE OF CONTENTS

LIST OF FIGURES

LIST OF TABLES

ACRONYMS

DECOVALEX	DEvelopment of COupled Models and their VAlidation against Experiments
DOE	Department of Energy
DPC	Dual Purpose Canister
EBS	Engineered barrier system
EDZ	Excavation damaged zone
FLAC	Fast Lagrangian analysis of continua
FY	Fiscal year
GDSA	Geologic Disposal Systems Analysis
LBNL	Lawrence Berkeley National Laboratory
PWR	Pressurized Water Reactor
SNF	Spent Nuclear Fuel
SNL	Sandia National Laboratories
SFWD	Spent Fuel and Waste Disposition
THM	Thermo-hydro-mechanical
TOUGH	Transport of Unsaturated Groundwater and Heat
UFD	Used Fuel Disposition
UFDC	Used Fuel Disposition Campaign
yOoR	years-Out-of-Reactor

This page is intentionally left blank.

1. INTRODUCTION

The report presents the progress of a newly initiated research activity addressing geotechnical and performance assessment impacts of direct disposal of commercial spent nuclear fuel (SNF) in dual-purpose canisters (DPCs) in various host rock environments. Previous studies on direct disposal of DPC within the Department of Energy's (DOE) Spent Fuel and Waste Disposition (SFWD) campaign found that direct disposal is technically feasible for most DPCs, depending on the repository host geology (Hardin et al., 2015). Post closure criticality control and thermal management strategies that allow for permanent disposal within 150 years (after taken out of the reactor) were identified as two of the most challenging aspects (Hardin et al., 2015). The DPCs are currently also being considered in the geologic disposal system analysis (GDSA) within the SFWD campaign. In GDSA, heat sources from either 24-PWR or 37-PWR DPCs are considered with a decay storage time varying from 50 to 150 years before disposal. The GDSA modeling is being conducted using large-scale models focusing on the radionuclide transport to accessible environments, and includes repository-scale coupled thermal-hydraulic processes. Previous studies on DPC thermal managements and the current GDSA work provide the basic background and a starting point for the current study on the geotechnical (or geomechanical) impact of direct DPC disposal.

Thermal management associated with geologic nuclear waste disposal is based on controlling the peak temperature in the bentonite buffer or in the rock wall. The same type of the thermal management should be performed in the case of DPC (Hardin et al., 2013; 2015). However, previous modeling studies have shown that in order to evaluate a geomechanical impact, the most critical is not the peak temperature of the waste canister, but the overall average and peak rock temperature at the repository level (e.g., Rutqvist et al., 2009a; 2014). The peak thermal stress on the repository tunnels occurs as a result of thermally-induced stress buildup at the repository level and associated stress concentration around the emplacement tunnel (Figure 1-1). For a repository in a low permeability host rock, such as argillite, salt, and crystalline rock, large scale pressure buildup may occur as a result of thermal expansion of trapped pore-fluids (Rutqvist et al., 2014). In this work, we investigate different peak temperature criteria (for buffer, rock wall and repository rock) related to the geomechanical impact for various rock environments.

Related to the clay-based buffer material, a peak temperature of 100 °C has frequently been adopted out of concern of chemical changes and degradation. For DPC direct disposal, a peak backfill temperature of 200 °C is likely to occur, unless the SNF is aged for hundreds of years before backfilling (Hardin et al., 2015). However, backfill peak temperature well above 100 °C is currently considered in national nuclear waste programs, such as in Switzerland, where *in situ* heater experiments up to 140 °C are being conducted for demonstration of the disposal concept in Opalinus Clay (Rutqvist et al., 2018; 2019). Moreover, the Clay-based backfill material such as bentonite-sand mixtures can be engineered to reduce the buffer peak temperature. For example, laboratory data have shown that the thermal conductivity of bentonite can be significantly increased by mixing in graphite or graphene oxide (Jobmann and Buntebarth, 2009; Chen et al., 2018). This shows the possibility of engineering a bentonite buffer in order to reduce the peak temperature exposed to the buffer during the post-closure period. The effect of such buffer material engineering is one of the aspects investigated in this work.

This report presents initial scoping calculations related to this newly initiated activity. The goal at this stage is not to make an exhaustive analysis of the problem, but to make an initial scoping calculation to identify some of the most important geomechanical impacts of direct disposal of SNF in DPCs. Previously developed and tested modeling approaches based on the TOUGH-FLAC simulator are applied with detailed representation of the near-field coupled processes (Rutqvist et al., 2011; 2014; 2019; 2018). The model setup is presented in Section 2, followed by thermal management calculations in Section 3, including a demonstration of the use of engineered buffer properties for reducing buffer peak temperature. In Section 4 THM responses for different DPC disposal options are modeled,

including disposal in 24 and 37-PWR DPCs, after 100 and 150 years-Out-of-the-Reactor (yOoR). The analysis is conducted for disposal in argillite and crystalline (granite) host rock in this initial study, while studies of other host rock environments will be conducted in future work.

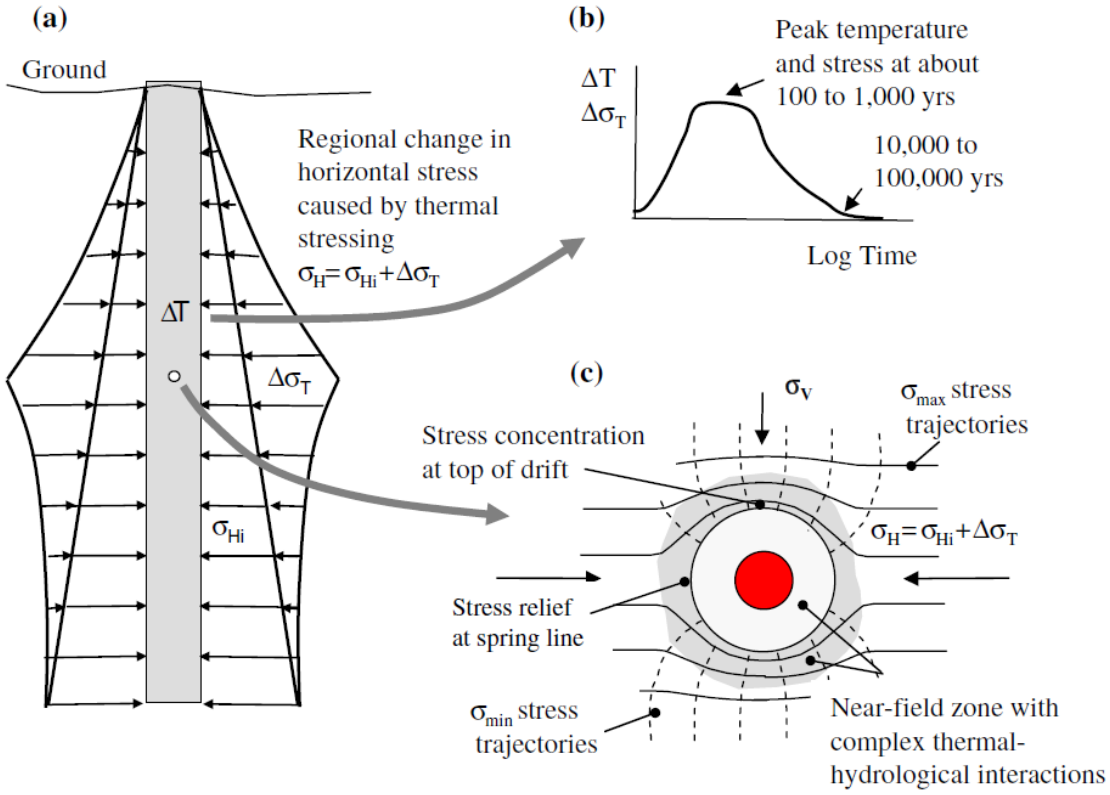

Figure 1-1. Schematic presentation of a conceptual model of thermally-induced stresses and mechanical impact on a nuclear waste emplacement tunnel based on coupled THM simulation results (Rutqvist et al., 2009a)

2. MODEL SETUP

The model setup and conditions for disposal in argillite and crystalline host rocks are conducted using similar geometry of the near field. That is, the DPCs (6 m long and 2 m in diameter) are placed on the floor of the emplacement tunnels of about 4.5 m in diameter (Hardin et al., 2013; 2014). The basic cross-section model of the emplacement tunnel is shown in Figure 2-1. Figure 2-1a presents a cross-section from Hardin et al. (2014), with the TOUGH-FLAC model geometry shown in Figure 2-1b for the backfilled emplacement tunnel in argillite. As suggested in Hardin et al., (2013), the sedimentary host rock option calls for reinforcement with a concrete liner and a concrete invert for placing the DPC. We assume a bentonite buffer backfill is from the FEBEX bentonite with properties similar to those we applied in previous generic modeling studies for crystalline and argillite repository concepts (Rutqvist et al., 2011; 2014). In the case of crystalline rock, we used the same model grid, but disregarded the concrete liner by assuming that those numerical grid-blocks belong to the host rock.

Figure 2-2 presents a three-dimensional symmetric model around one DPC with a canister-to-canister spacing of 20 m along the emplacement tunnels and a 40 m spacing between individual emplacement tunnels. In this modeling study, the dimensions are fixed to those given in Figure 2-2, and disposal at a 500-meter depth is assumed. In addition to the three-dimensional model shown in Figure 2-2, we also conducted simulations in a two-dimensional cross-section, for faster executions of simulations over 100,000 years. For simplicity and computational speed, stress-strain evolution is calculated considering linear elastic properties in these preliminary simulations. The calculated stress field are then integrated with basic failure criteria to evaluate the potential for damage and to determine what types of damage are most likely to occur, if any, for different types of host rock and DPC disposal options.

Material properties of both argillite and crystalline host rocks are assumed isotropic. The material properties for the argillite repository case are the same as those used in Rutqvist et al. (2014), representing Opalinus Clay at the Mont Terri laboratory, Switzerland, and the FEBEX bentonite properties, given in Rutqvist et al., (2011). A simple swelling model is used, as described in Rutqvist et al. (2011), to provide a 5-MPa swelling stress upon full saturation of bentonite. The thermal conductivity of the bentonite buffer is linearly dependent on saturation varying from λ_{dry} = 0.5 W/mK (at zero liquid saturation) to λ_{wet} = 1.3 W/mK (at full liquid saturation). For the crystalline rock case, granitic rock properties are taken from previous coupled processes modeling studies within the international DECOVALEX project (Rutqvist et al., 2009a; Nguyen et al., 2009; Rutqvist et al., 2009b). Those properties were derived from site investigations at the Äspö Hard Rock Laboratory in Sweden and the Manitoba Underground Research Laboratory in Canada. The basic THM properties are listed in Table 2-2.

For initial conditions, hydrostatic fluid pressure and a thermal gradient of 28 °C per km are assumed. With the ground water table near the ground surface and a ground surface temperature of 10 °C, the initial pressure and temperature at 500 m depth is about 4.5 MPa and 24 °C. Isotropic stress field is assumed with the magnitude of three principal stresses being equal to the weight of the overburden rock, leading to a slightly higher initial stress in the case of crystalline rock.

The modeling steps include excavation, reinforcement, emplacement of the waste canisters and a buffer, followed by the post-closure simulation over 100,000 years (Figure 2-3). In the simulation of an argillite repository tunnel, a concrete liner is assumed be installed during the excavation, assuming no convergence of the softer argillite host rock by the stiffer and stronger concrete liner. It is also assumed that the DPC and a buffer are installed at an instant defined as time zero in the post-closure simulations. The buffer is installed at an initial saturation of 65%. In the case of crystalline (granite) host rock, no concrete liner is installed. As mentioned, simulations were conducted using several options of heat power decay function, including both 24-PWR or 37-PWR DPCs with a decay storage of up to 150 years before disposal.

In the post-closure simulations, the potential geomechanical impact is evaluated in terms of the stress evolution at the repository level and at the tunnel wall. The stress-strain evolution is calculated considering

linear poro-elasticity and thermo-elasticity, whereas the potential for failure is considered through some simple stress criteria. For the repository level stresses, a simple criterion is that a tensile stress equals to or larger than a tensile strength causing tensile failure, while a shear stress equals to or larger than a shear strength (such as a maximum compressive stress being 3 times that of the minimum compressive stress), which would cause shearing of pre-existing fractures (Rutqvist et al., 2014). For the top and bottom of the tunnel, where the highest compressive tangential stress is expected to occur, a spalling failure criterion is considered through a uniaxial compressive strength. According to site investigations at Manitoba URL in Canada and at Äspö hard rock laboratory in Sweden, a so-called spalling strength of about 120 MPa has been estimated (Rutqvist et al., 2009c). For Opalinus Clay, we use the uniaxial compressive strength of about 16 MPa, which was determined by laboratory experiments (Rutqvist et al., 2014). On the sidewalls of the tunnel, there will be a relief of tangential compressive stress (Figure 1-1), which could potentially lead to development of a large tensile stress, resulting in tensile fracturing.

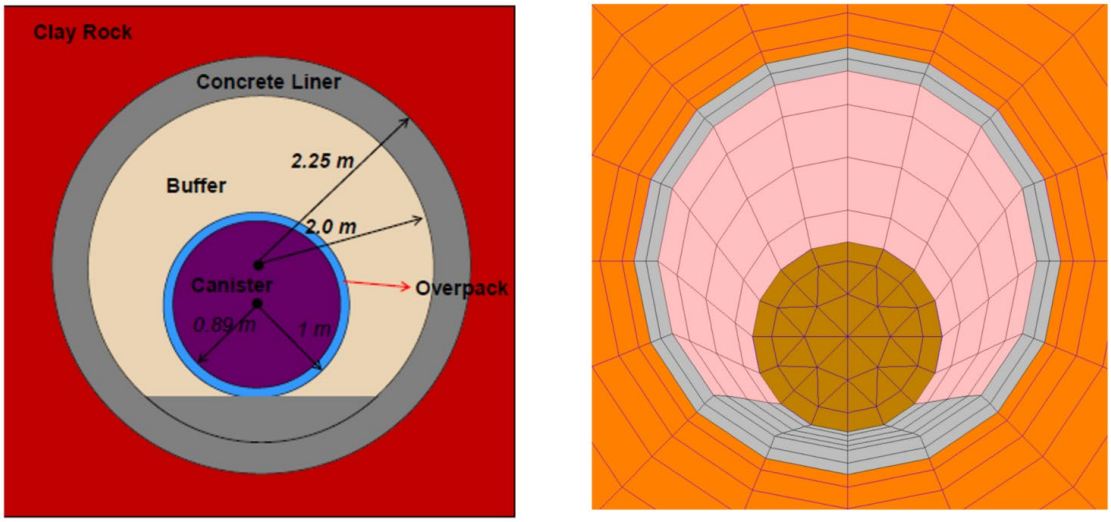

Figure 2-1. EBS geometry considered in this study for direct disposal of DPC in a horizontal emplacement tunnel with the DPC placed on a concrete invert at the bottom of the tunnel: (a) geometry for an emplacement tunnel in sedimentary rock (Hardin et al., 2014), and (b) numerical grid of the near field.

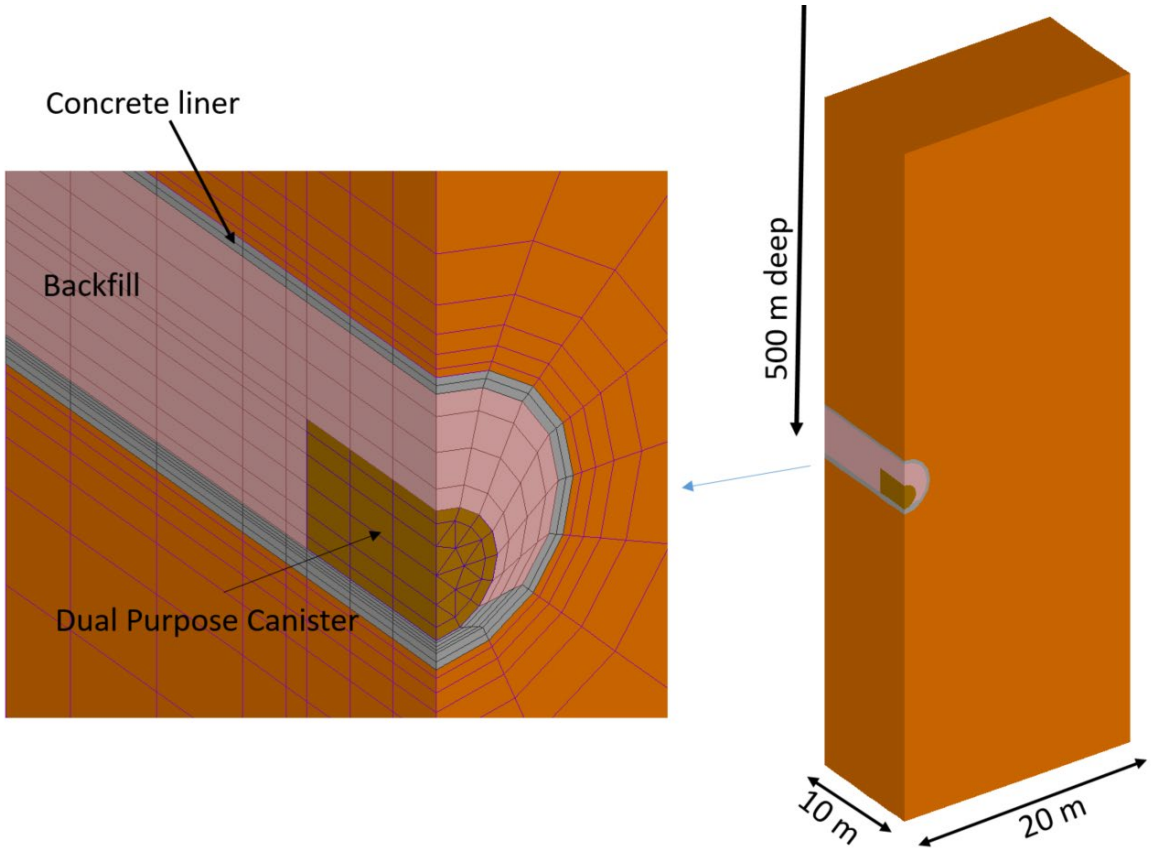

Figure 2-2. Three-dimensional model geometry of a horizontal emplacement tunnel in the middle of the repository with 20 m center-to-center spacing between individual DPCs and 40 m spacing between individual emplacement tunnels.

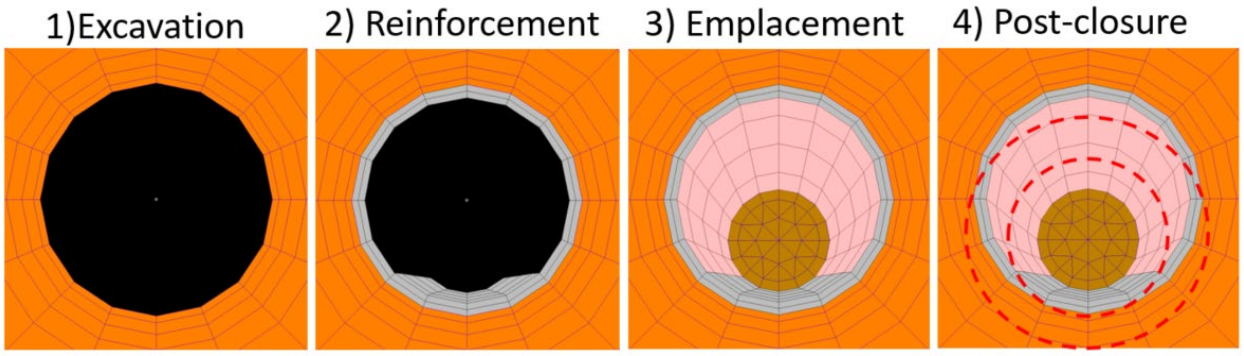

Figure 2-3. Modeling steps: from tunnel excavation to post-closure periods.

Table 2-1. Basic THM properties

Parameter	Argillite (Opalinus Clay)	Crystalline (Granite)	Concrete
Bulk Density [kg/m^3]	2400	2700	2700
Porosity [-]	0.15	0.01	0.15
Young's Modulus [GPa]	5	35 (fractured) 60 (intact)	23
Poisson's ratio [-]	0.3	0.3	0.2
Grain Specific heat [J/kg·°C]	900	900	900
Thermal conductivity [W/m·°C]	1.7	3.0	2.0
Thermal expansion coefficient [°C^{-1}]	1.0×10^{-5}	1.0×10^{-5}	1.0×10^{-6}
Bulk Permeability [m^2]	5.0×10^{-20}	1.0×10^{-17} (fractured) 1.0×10^{-19} (intact)	1.0×10^{-19}

3. THERMAL MANAGEMENT FOR BUFFER AND HOST ROCK

We first present results of basic high-temperature thermal-hydraulic responses based on the results of simulations using the full three-dimensional model shown in Figure 2-2. This model enabled us to study more accurately the temperature evolution in the buffer and surrounding rocks, considering the detailed near-field geometry with a DPC placed at the tunnel floor on a concrete invert. We also conducted a sensitivity study of how admixtures of high thermal conductivity materials to the bentonite could improve the thermal performance and reduce the peak temperature at the buffer during the post-closure period.

3.1 Basic Thermal-Hydraulic Response

Figure 3-1 presents the graphs of the evolution of temperature, buffer saturation and fluid pressure calculated for a repository in argillite with 24-PWR DPC, emplaced 100 yOoR. The temperature at the interface between the canister and buffer peaks at 150°C within 10 years, and stays well above 100°C for up to 1000 years. The temperature at the rock wall peaks at 104°C after 300 years, whereas the rock temperature at mid-distance between two emplacement tunnels peaks at 85°C after 750 years (Figure 3-1a). The buffer experiences significant drying at its inner parts near the canister during the first tens of year, and the buffer finally saturates fully after 75 years (Figure 3-1b).

Fluid pressure increases as a result of thermal pressurization, a phenomenon known to occur when heating pore-fluids in low permeability rocks, such as shale (Rutqvist et al., 2014). The pressure peaks at 14.6 MPa after about 1000 years (Figure 3-1c). The thermal pressurization is driven by temperature changes in the host rock away from the emplacement tunnel and peaks a few hundred years after the host rock temperature peaks. In this case, the weight of the overburden rock at 500 m depth results in 11.8 MPa vertical stress (lithostatic stress). The thermally-driven increase in fluid pressure exceeds the vertical stress by several MPa and it is therefore a significant risk for hydraulic fracturing taking place over the entire repository horizon. The only way to prevent such a high fluid pressure would be to design the repository with proper control of the host rock temperature.

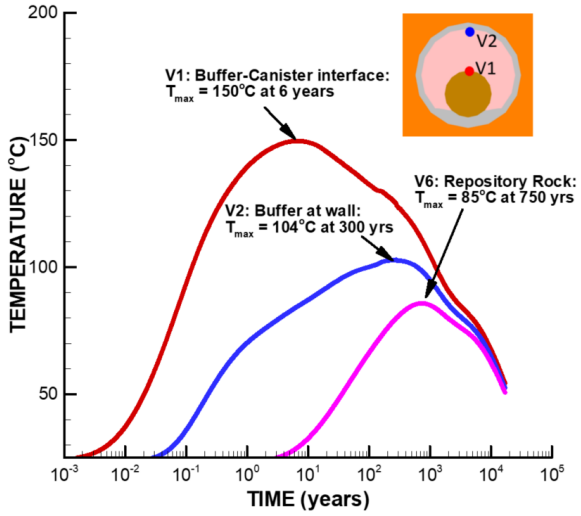

(a)

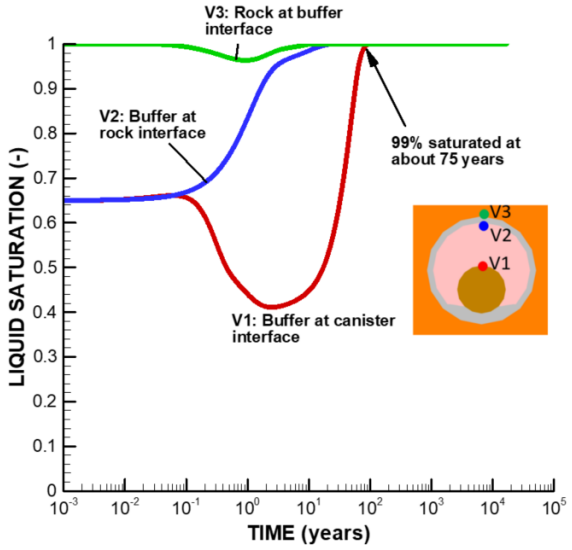

(b)

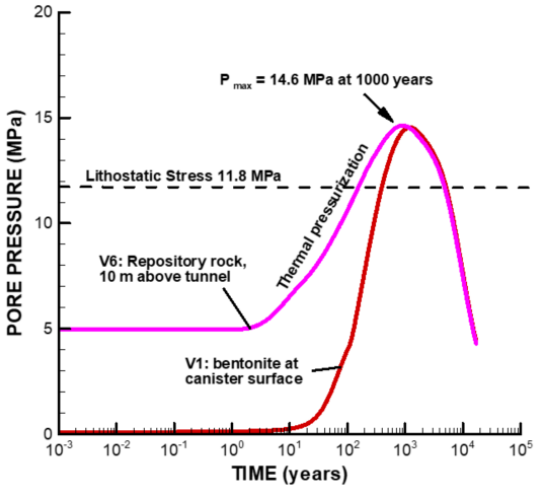

(c)

Figure 3-1. Thermal-hydraulic simulation results for a repository in argillite considering a heat source from a 24PWR-100yOoR DPC: Evolution of (a) temperature ,(b) saturation and ,(c) pore pressure

3.2 Engineered Buffer Thermal Properties to Reduce Temperature

Figure 3-2 and 3-3 present the results of using engineered buffer material to reduce the peak temperature and thermal impact. Two cases of enhance thermal properties are considered based on literature laboratory data on bentonite thermal conductivity for different engineered admixtures.

Firstly, we consider thermal conductivity values from Jobmann and Buntebarth (2009), for 15% graphite added to the bentonite, resulting in h λ_{dry} = 2.0 W/mK and λ_{wet} = 3.2 W/mK. This is significantly higher

thermal conductivity than the original values of λ_{dry} = 0.5 W/mK and λ_{wet} = 1.3 W/mK. The calculation results are shown in Figure 3-2.

Secondly, a more extreme case is considered based on newly published laboratory results in Chen et al., (2018). In this case, thermal conductivity of bentonite could be increased by an order of magnitude using admixtures of graphene oxide. For example, with 30% graphene oxide, λ_{dry} = 5 W/mK and λ_{wet} could be estimated to exceed 25 W/mK. Here we use λ_{dry} = 5 W/mK and λ_{wet} =10 W/mK, which is much higher than the thermal conductivity of the Opalinus Clay host rock (λ_{dry} = 1.7 W/mK). And the calculation results are shown in Figure 3-3.

The results in Figures 3-2 and 3-3 show the benefit of such an engineered buffer material. In this example, the peak temperature reduced from 150°C to 115°C or to 104°C depending on the thermal conductivity of the buffer. Moreover, the thermal gradient across the buffer is substantially reduced, which has the benefit of preventing drying of the buffer next to the heater. For example, from Figure 3-3b we can see that in the base case, the water saturation decreases from 65% to 40% (dashed red line in Figure 3-3b), while for the case with high buffer thermal conductivity, saturation decreases only a few percent (solid red line in Figure 3-3b).

Another observation from Figures 3-2 and 3-3 is that the temperature evolution in the repository host rock is unchanged and does not depend on the thermal conductivity of the buffer. This also means that the thermal pressurization effects are identical for the different cases of buffer thermal conductivity (as shown in Figure 3-4). Thus, the host rock temperature change and associated thermal pressurization would still be too high as the pressure at times exceeds the lithostatic stress and could cause hydraulic fracturing of the host rock.

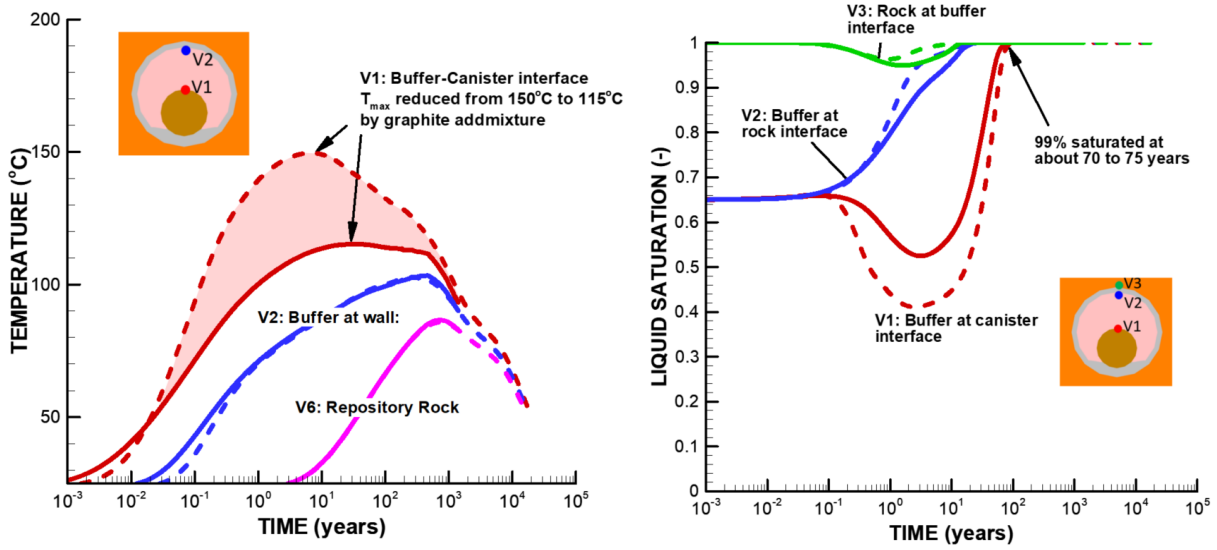

(a) (b)

Figure 3-2. Effect of 15% graphite admixture in the bentonite buffer material to enhance thermal conductivity and reduced peak temperature (heat source from a 24PWR-100yOoR DPC): (a) temperature evolution and (b) evolution of liquid saturation. Dashed lines are the results for the original unmodified bentonite thermal properties and solid lines are the results for enhanced thermal conductivity.

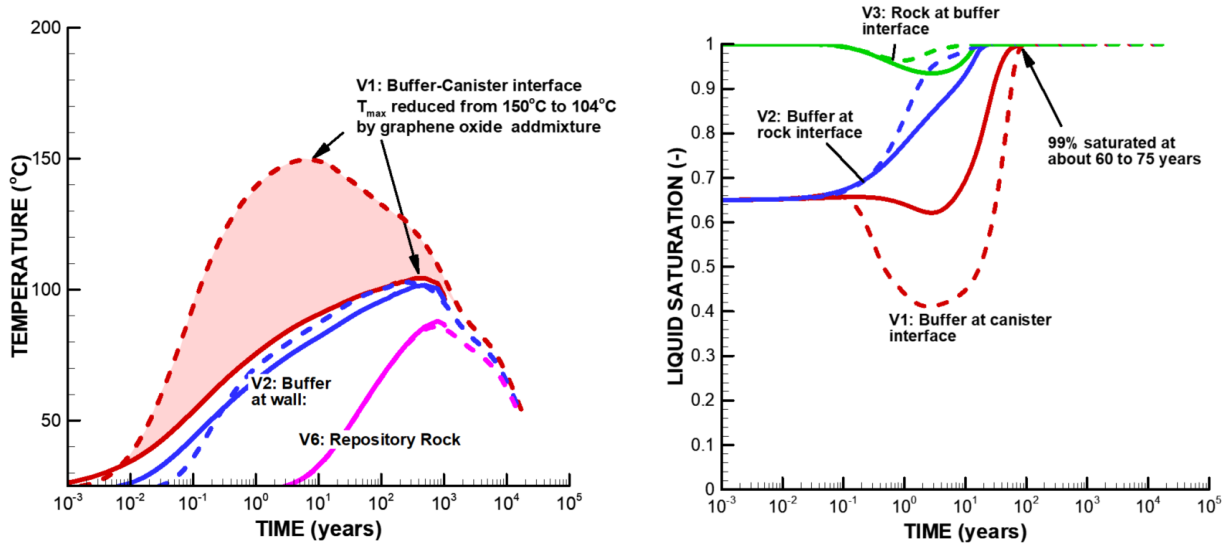

(a) (b)

Figure 3-3. Effect of 30% graphene oxide admixture to bentonite buffer material to enhance thermal conductivity and reduced peak temperature (heat source from a 24PWR-100yOoR DPC): (a) temperature evolution and (b) evolution of liquid saturation. Dashed lines are the results for the original unmodified bentonite thermal properties and solid lines are the results for enhanced thermal conductivity.

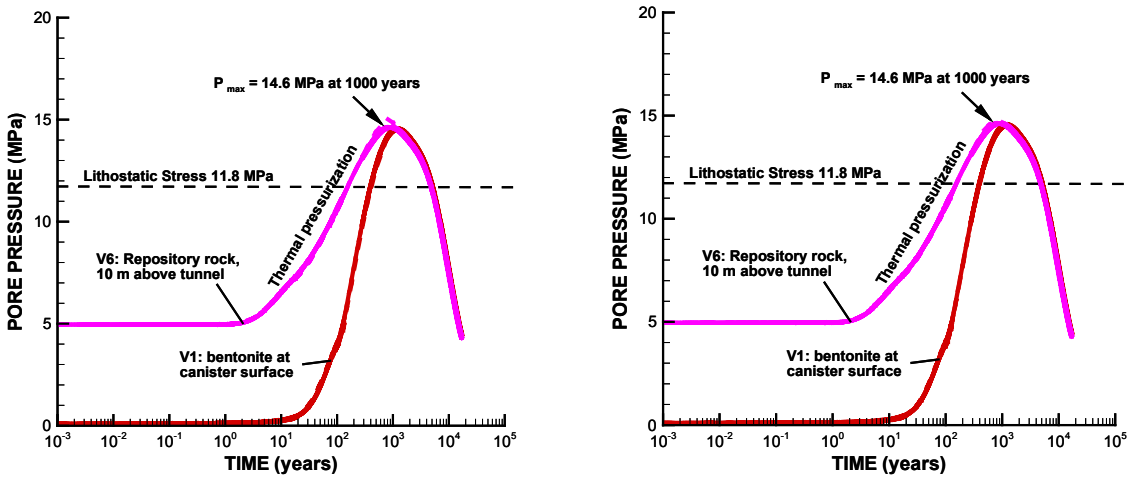

(a) (b)

Figure 3-4. Pore pressure evolution for the two cases of (a) adding 15% graphite in the bentonite buffer and (b) adding 30% graphene oxide admixture. The results for the original and enhanced thermal conductivity cases (sold and dashed lines) are indistinguishable because the thermal conductivity of the buffer has no significant impact on the temperature evolution in the host rock.

4. HIGH-TEMPERATURE THM RESPONSES

High-temperature THM responses are investigated for a number of cases considering argillite (Opalinus Clay) and crystalline (granite) host rocks. In all cases, the repository emplacement tunnels are assumed to be located at 500 m depth. The same near-field geometry is assumed, but in the case of a repository tunnel in Argillite, a concrete liner is considered for necessary reinforcement, whereas in the case of granite, it assumed that a concrete liner is not required (Figure 4-1).

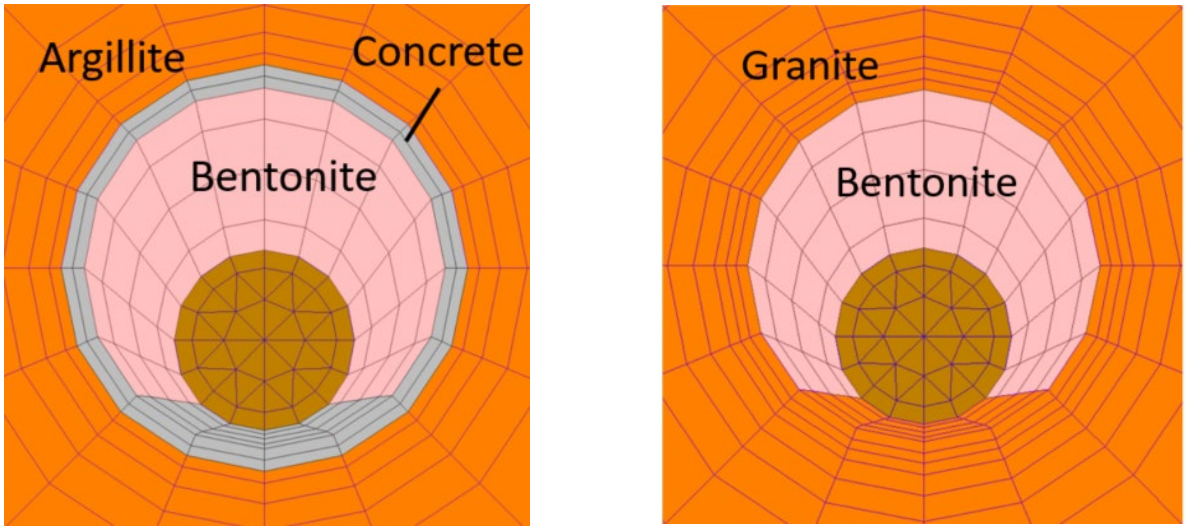

(a) (b)

Figure 4-1. Modeled EBS geometry for the cases of a repository tunnel located in (a) argillite (Opalinus Clay) and (b) crystalline (granite) host rock.

4.1 2D Thermal Line Load

The TOUGH-FLAC simulation for investigating THM responses is conducted on a 2D cross-section model, which is an approximation compared to the full 3D model presented in Section 3. In order to run a reasonable simulation, we need to choose an appropriate line thermal load, i.e. thermal heat power for the 2D cross-section that could accurately represent the real three-dimensional temperature evolution. A low limit line load per meter emplacement tunnel can be estimated from total power of one waste package, divided by the spacing (center-to-center) between each waste package along the emplacement tunnels. For example, a 24PWR DPCs 100 yOoR and 20 m DPC spacing, result in an initial heat power of 3881 W/ 20 m = 194 W/m. A high limit could be calculated based on the length of the canisters, i.e. 3881 W/ 6 m = 647 W/m. The high limit of 647 W/m matches the first few year of heating close to the canister, but overestimates the peak load in the rock over the longer term. For this study on the geotechnical impact, the temperature evolution in the rock is most relevant, so we used a compromise, which correspond to 194 W/m multiplied by a factor of 1.2, i.e. 233 W/m of the initial heat power.

Figure 4-2 shows a comparison of the full 3-D and 2-D modeling results. We can see that the peak temperature and a temperature evolution in the rock are almost the same for 3-D and 2-D simulations. Thus, we assumed we could apply the 2-D model to study coupled THM processes to determine the main impacts on the geotechnical performance.

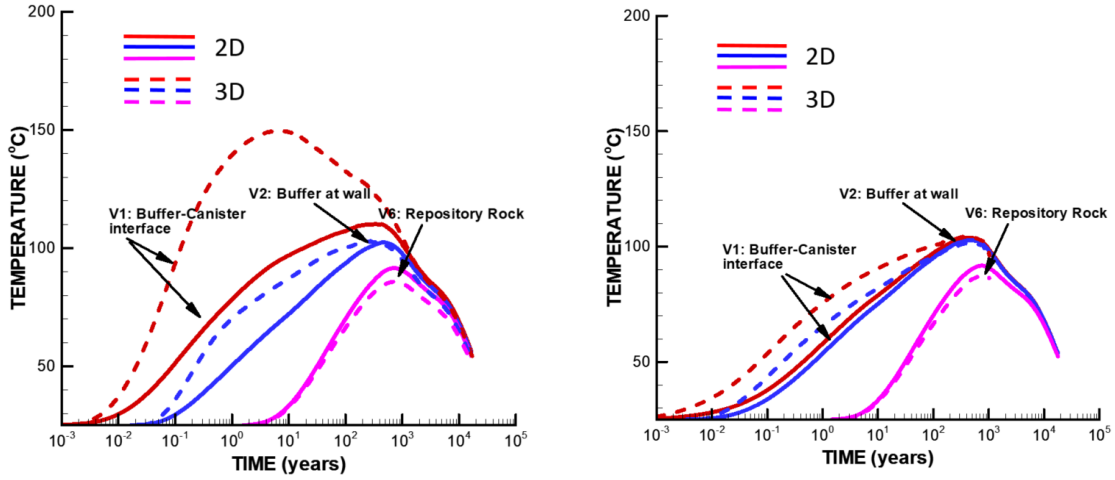

Figure 4-2. Comparison of simulated temperature evolution for a full 3-D model with a 2-D cross-sectional model for a calibrated 2-D line heat source for a representation of the temperature evolution in the host rock. Results are for (a) original bentonite thermal conductivity, and (b) enhanced thermal conductivity by 30% graphene oxide admixture.

4.2 THM Response in Argillite Host Rock with 24PWR DPCs

The THM responses around an emplacement tunnel in argillite host rock with DPCs containing 24PWR 100 yOoR are depicted in Figures 4-3 through 4-6. The graphs of temperature and pressure evolution shown in Figure 4-3 are the same as those for the 2-D cases in Figure 4-2. That is, the thermal pressurization and the associated pressure evolution are induced by and proportional to the temperature evolution in the host rock.

Figure 4-4 presents the graphs of the evolution of vertical and horizontal stresses at a point located at the mid-distance between two emplacement tunnels, and, therefore, representing the general repository stress. In Figure 4-4, both total and effective stresses are presented, and the difference between the total and effective stresses is the fluid pressure. The total vertical stress is approximately constant and equals to the weight of the overburden rock, which is about 11.8 MPa (Figure 4-4a). The increase in the fluid pressure causes a reduction in the vertical effective stress, which becomes tensile at about 100 years. Such tensile effective vertical stress is expected to last for several thousand years, and could cause massive tensile fracturing. The horizontal total stress increases with fluid pressure, resulting in the pore-elastic stress between the confined lateral boundaries (the model cannot expand in the horizontal direction and instead horizontal stress increases with increasing temperature and pressure). This leads to small changes of the horizontal effective stress.

Figures 4-5 and 4-6 present the graphs of the evolution of stresses at the wall of the tunnel within the inner part of the concrete liner (Figure 4-5) and in the host rock just outside of the concrete liner (Figure 4-6). After excavation and emplacement of the concrete liner, the stiffer concrete liner prevents further convergence of the softer argillite host rock, leading to a compressive tangential stress of up to 40 MPa in the concrete liner. The radial stress is much smaller due to the free surface to the tunnel opening that is filled with bentonite, where the initial stress is low. During the post-closure period, the tangential stress in the concrete liner is reduced, and a very high tensile effective stress occurs at the side of the tunnel. This high tensile stress would certainly cause tensile failure of the concrete liner that could potentially expand

out into the host rock. In simulations, we assumed a linear elastic constitutive behavior, whereas if tensile failure is considered, the tensile stress could not increase as high as shown in Figure 4-5b. The stress in the argillite host rock shown in Figure 4-6 is smaller, though the magnitude of tangential stresses is close to the uniaxial compressive strength of Opalinus Clay. However, the concrete liner provides confinement with a confining stress of several MPa, and, therefore, rock failure may be minimal. In reality, the concrete liner may disintegrate over time, and, therefore, it is not considered in the current analysis.

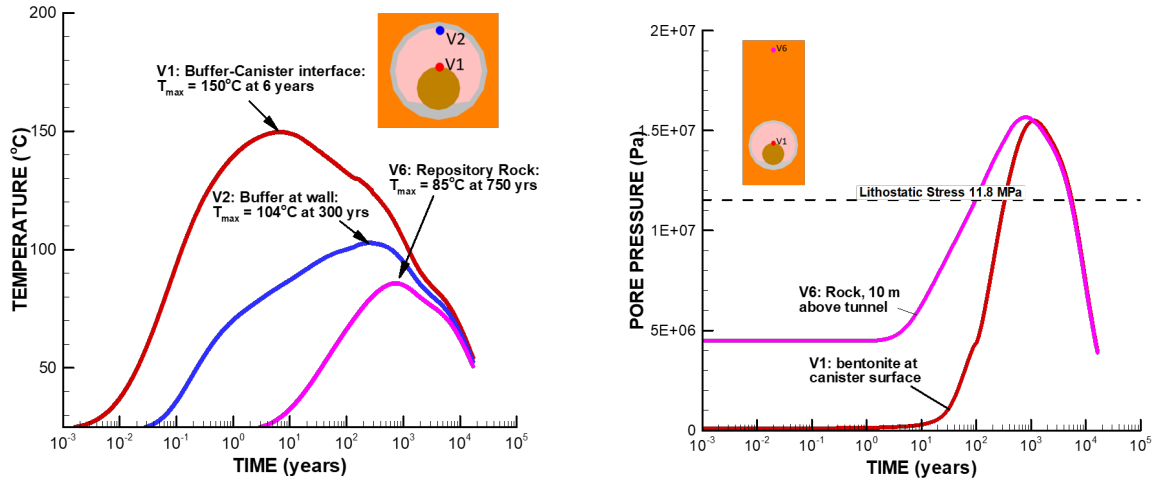

(a) (b)

Figure 4-3. Results of temperature (a) and pore pressure (b) thermal-hydraulic simulations for a repository tunnel in argillite (thermal line load from a 24PWR-100yOoR DPC).

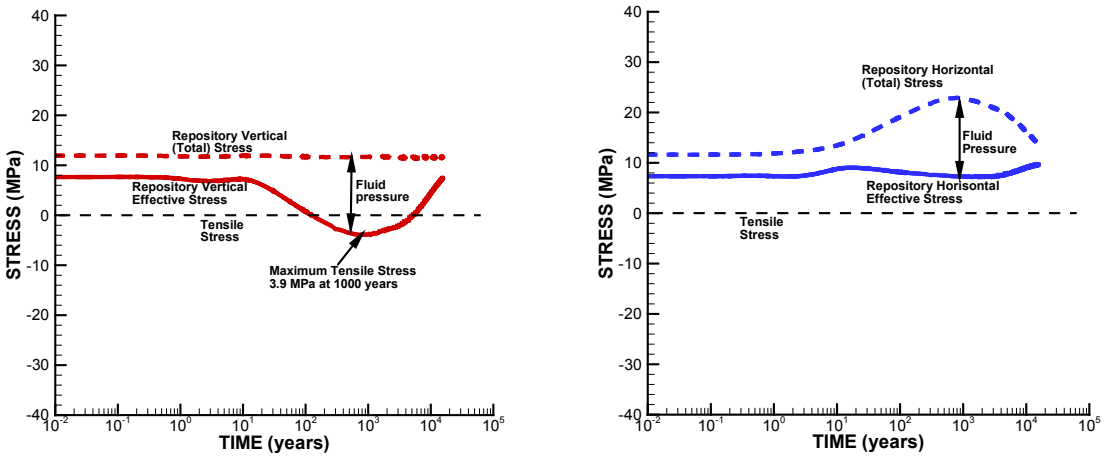

(a) (b)

Figure 4-4. Results of simulations of vertical (a) and horizontal (b) stresses for a repository tunnel in argillite (thermal line load from a 24PWR-100yOoR DPC). Dashed lines are total stresses, and solid lines are effective stresses.

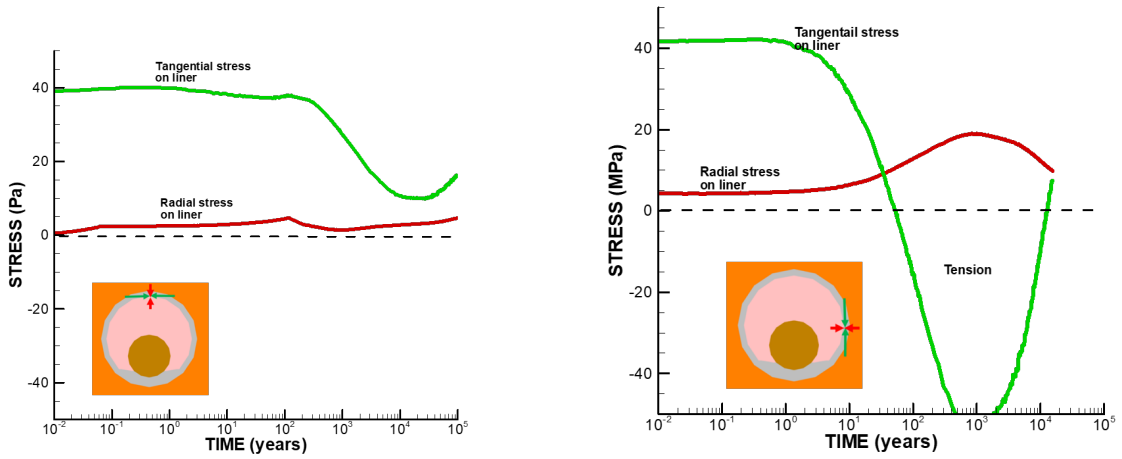

(a) (b)

Figure 4-5. Results of simulations of the evolution of stresses within the concrete liner: (a) at the top of the tunnel, and (b) at the side of the tunnel, for a repository tunnel in argillite (thermal line load from a 24PWR-100yOoR DPC).

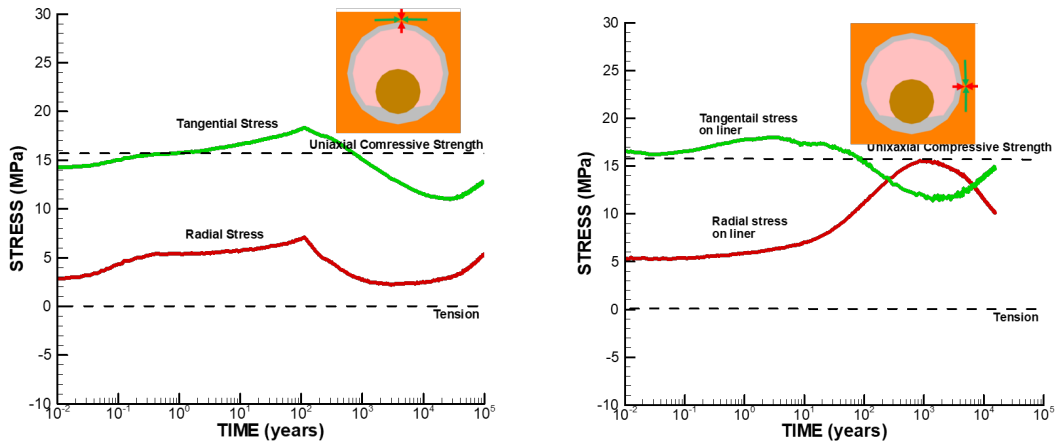

(a) (b)

Figure 4-6. Results of simulations of the evolution of stresses in the wall rock just outside the concrete liner: (a) at the top of the tunnel, and (b) at the side of the tunnel, for a repository tunnel in argillite (thermal line load from a 24PWR-100yOoR DPC).

4.3 THM Response in Argillite Host Rock with 37PWR DPCs

For a sensitivity study of the impact of heat load, the case of a higher heat load with 37PWR DPCs is considered. Moreover, two cases of surface thermal decay storage times are considered by employing the heat load for 37PWRs with emplacement 100 and 150 yOoR.

Figure 4-7 shows the results of temperature and pressure simulations, indicating that the time out of the reactor, 100 or 150 years, has the highest impact on the early time temperature evolution, especially in the buffer, whereas the rock mass temperature away from the emplacement tunnel (purple line in Figure 4-7a) are less impacted. In both cases, the peak temperature in the host rock is very high, reaching about 140 to 150°C, and the associated thermal pressurization results in a very high pressure that far exceeds the lithostatic stress (Figure 4-7b).

Figure 4-8 shows the associated evolution of vertical and horizontal stresses at the repository level. As a result of the high pressure increase due to thermal pressurization, the effective vertical stress becomes tensile within 10 years, and remains tensile for up to 10,000 years. The peak tensile stress of 15 to 20 MPa would in reality cause hydraulic fracturing, though this has not been modeled in this linear elastic analysis.

Figures 4-9 and 4-10 show the impact of the stress evolution near the tunnel wall. The results for 37PWR shown in Figures 4-9 and 4-10 are qualitatively similar to those of 24PWR in Figures 4-5 and 4-6, but the magnitudes of stress changes are much larger due to the higher heat load from 37PWR canisters. Another important observation from Figures 4-9 and 4-10 is that the surface heat decay storage, with disposal at 150 or 150 yOoR, has a relative small impact on the stress evolution. Thus, based on simulations of the geomechanical impact, longer surface heat decay storage does not significantly improve the DPC performance.

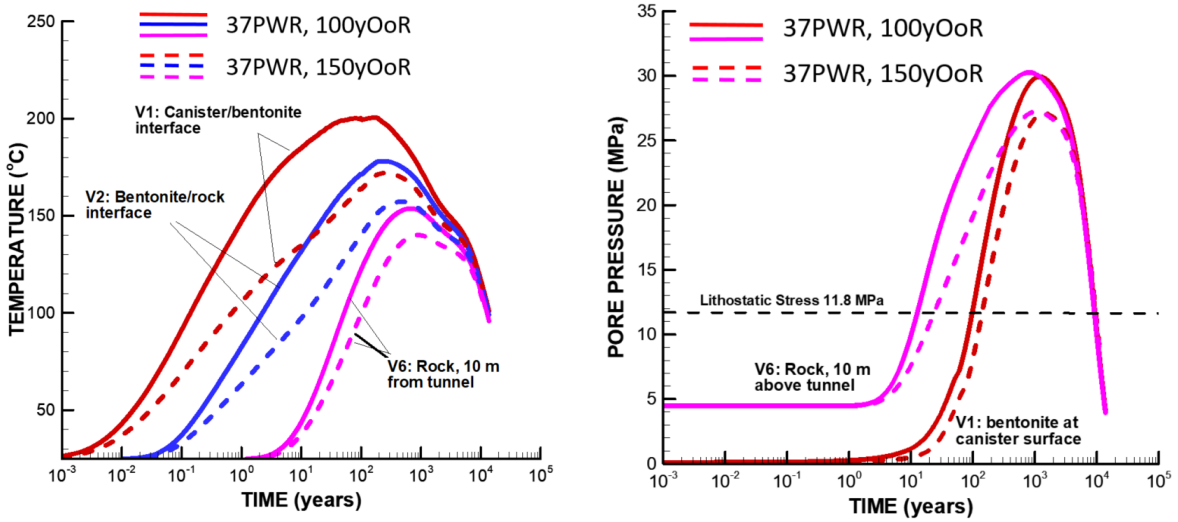

(a) (b)

Figure 4-7 Results of simulations of (a) temperature and (b) pore pressure, demonstrating the impact of surface heat decay storage time (disposal at 100 or 150yOoR for a 37PWR DPC) on the thermal-hydraulic response for a repository tunnel in argillite.

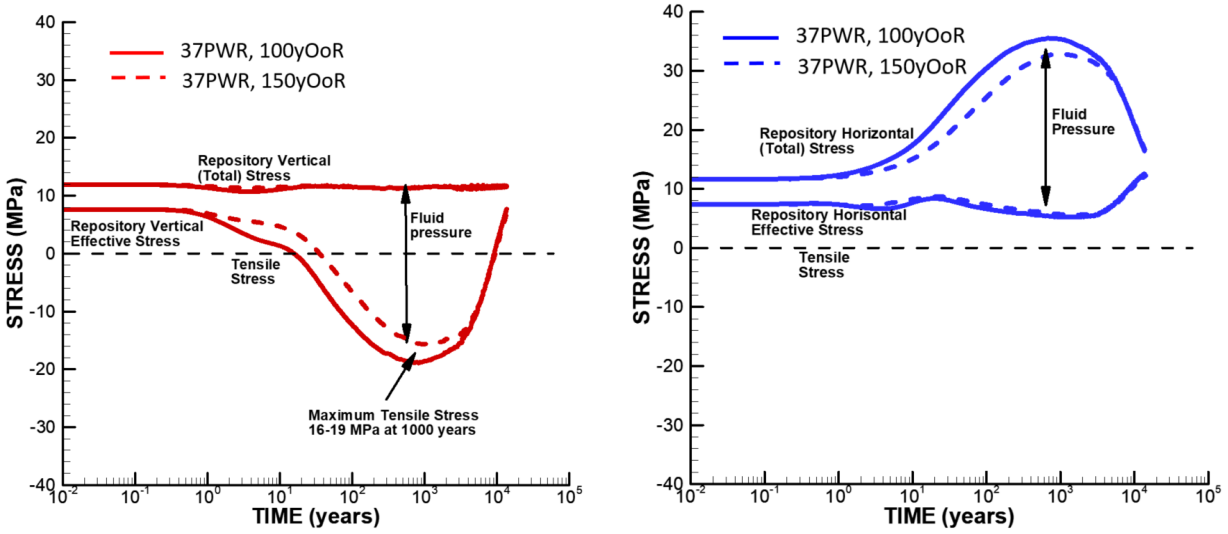

(a) (b)

Figure 4-8. Results of simulations of (a) vertical, and (b) horizontal stresses for a repository tunnel in argillite (thermal line load from a 37PWR-DPC emplaced at 100 or 150yOoR).

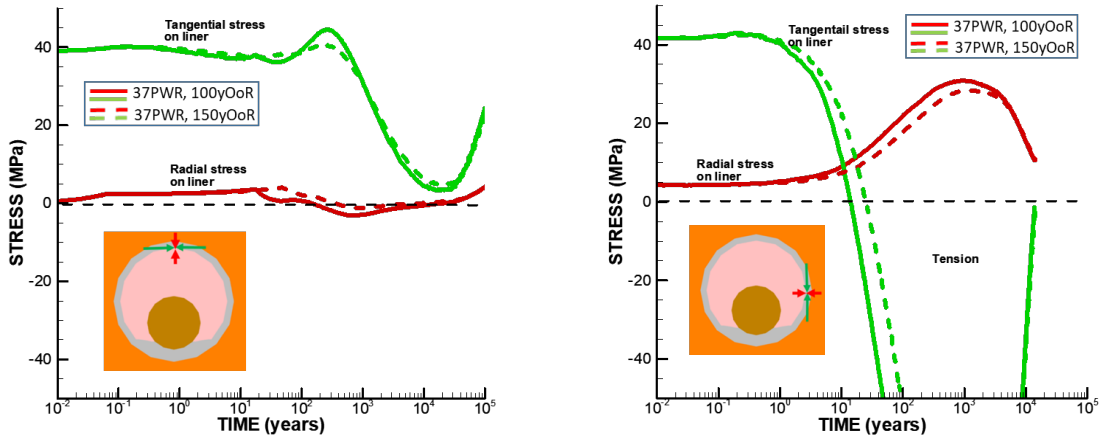

(a) (b)

Figure 4-9. Results of simulations of stresses within the concrete liner: (a) at the top of the tunnel, and (b) at the side of the tunnel, for a repository tunnel in argillite (thermal line load from a 37PWR-DPC emplaced at 100 or 150yOoR).

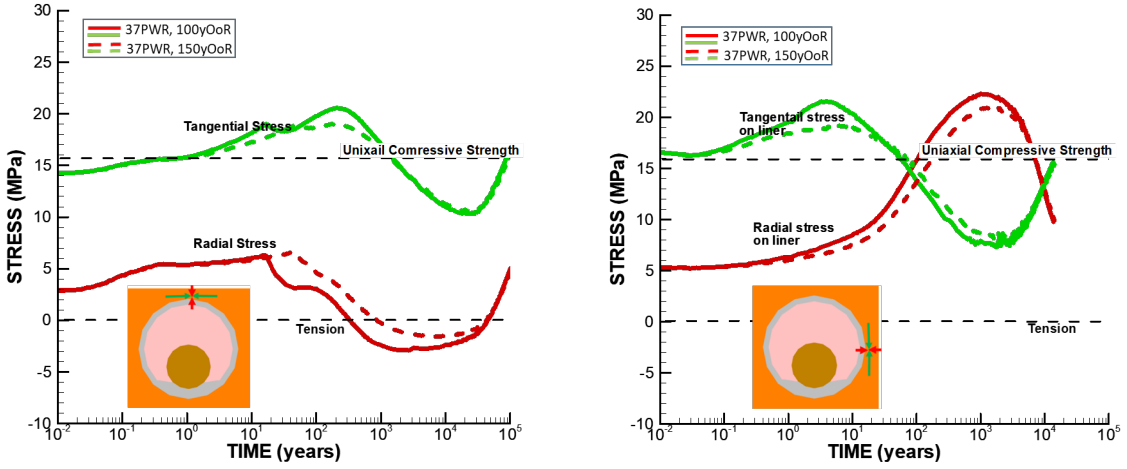

(a) (b)

Figure 4-10. Results of simulations of stresses in the wall rock just outside of the concrete liner: (a) at the top of the tunnel, and (b) at the side of the tunnel, for a repository tunnel in argillite (thermal line load from a 37PWR-DPC emplaced at 100 or 150yOoR).

4.4 THM Response in Fractured Granite with 37PWR DPCs

In the case of fractured granite, we considered rock characteristics somewhat similar to those at the Äspö Hard Rock Laboratory, Sweden. In this case, permeability is much higher than that of intact granite and the Young's modulus of the rock mass is smaller than that for intact (unfractured) granite. The permeability is set to 1×10^{-17} m^2, and the Young's modulus of the rock mass is set to 35 MPa (Rutqvist et al., 2009a). The thermal conductivity is set to 3.0 W/mK, which is almost twice as high as that for the argillite case presented in Section 3 of this report.

In terms of THM responses, the main difference for the fractured granite case compared to the argillite case is the thermal pressurization is much smaller, but thermal stresses are much higher. The peak temperature in the host rock in this case for 100 yOoR is about 115 °C, which is much lower than the 150°C that was calculated in the case of argillite (compare peak temperatures in Figures 4-7a with 4-11a). Thermal pressurization is not shown in Figure 4-11b, because it quickly diffuses any pressure buildup due to the high rock permeability.

The rock stress evolution at the repository level (as shown in Figure 4-12) for fractured granite is quite different from that in argillite (as shown in Figure 4-8). The main mechanical response for the fractured granite case is an increase in the horizontal stress caused by a thermal stress due to temperature changes in the host rock. An increase in the horizontal stress causes an increase in differential (shear) stress. If the shear stress is sufficiently large, shear activation of pre-existing fractures and/or faults could occur, if they are oriented along the shear activation in the disturbed stress field. A simple criterion for potential shear activation of a fracture is: a maximum compressive effective stress is 3 times larger than the minimum compressive effective stress (Rutqvist et al. 2014). In this case, the minimum compressive effective stress remains practically constant at about 10 MPa (Figure 4-12a), and, therefore, shear activation could be possible if the maximum principal stress exceeds 30 MPa. The 30 MPa maximum compressive stress criterion is marked with a dashed line in Figure 4-12b. The horizontal compressive stresses exceed 30 MPa after about 20 to 50 years, and remain above 30 MPa for up to 10,000 years. High shear stress prolonged

for such a long time in a fractured rock mass could certainly have the potential for induced shear activation and, perhaps, induced seismicity.

The rock mass horizontal thermal stress will cause strong stress changes at the tunnels walls as shown in Figure 4-13. At the top of the tunnel, the thermal horizontal stress and stress concentration around the tunnel cause the compressive stress to increase and peak at 128 MPa for the case of 37PWR 100yOoR. Such a high compressive tangential stress is close to the spalling strength observed in granite at the Äspö Hard Rock Laboratory. However, those values are for unsupported tunnel walls, whereas in this case a support stress has already been developed by the swelling stress in the buffer. As observed in Figure 4-13a, the radial stress has increased to 5 to 10 MPa, and, therefore, the tangential stress of 128 MPa would not likely induce any significant damage to the host rock. Also at the side of the tunnel, the stresses are relatively small, but with some potential tension in the tangential stress (Figure 4-13b).

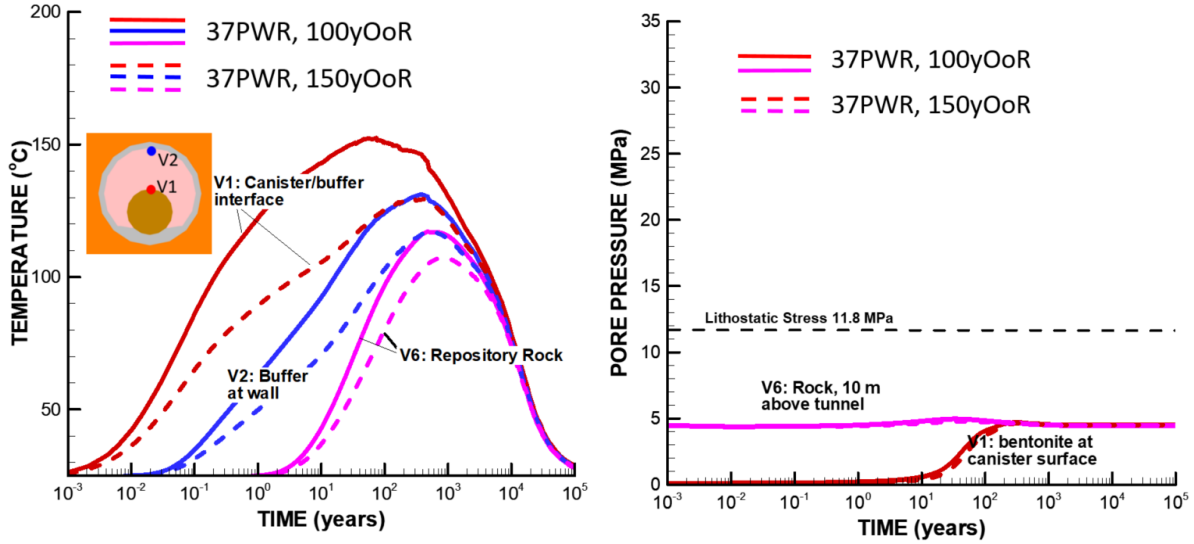

(a) (b)

Figure 4-11. Results of simulations of (a) temperature, and (b) pore pressure, demonstrating the impact of surface heat decay storage time (disposal at 100 or 150yOoR for a 37PWR DPC) on the thermal-hydraulic response for a repository tunnel in fracture granite.

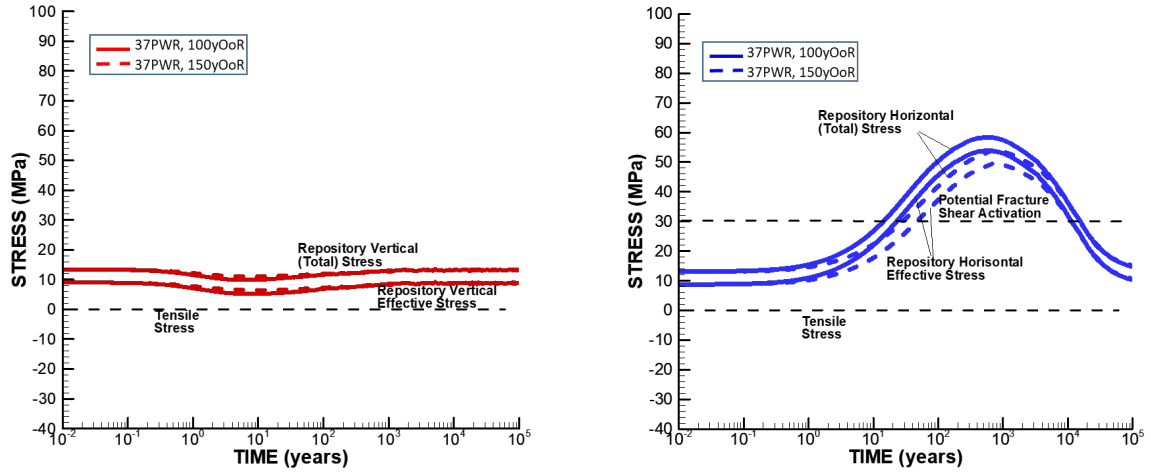

(a) (b)

Figure 4-12. Results of simulations of (a) vertical, and (b) horizontal stresses for a repository tunnel in fractured granite (thermal line load from a 37PWR-DPC emplaced at 100 or 150yOoR).

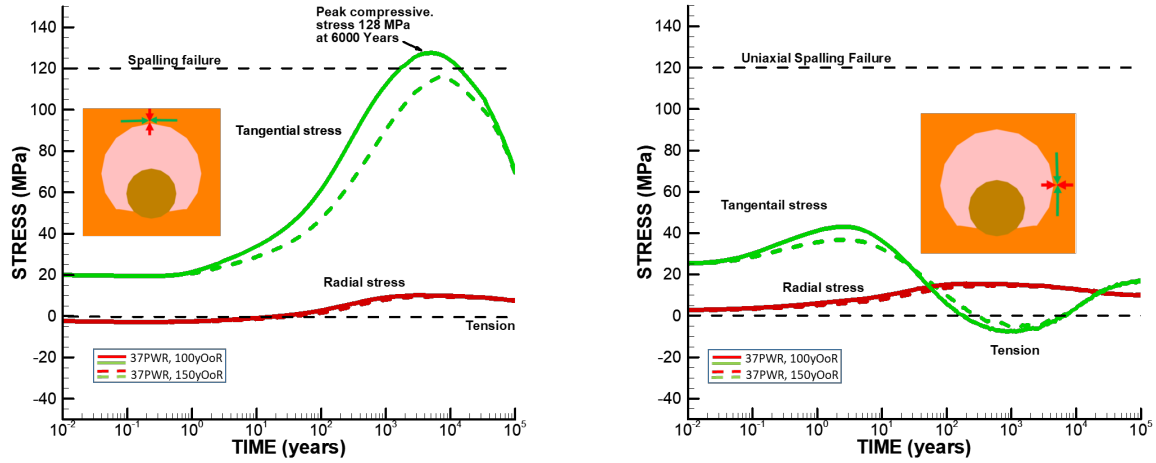

(a) (b)

Figure 4-13. Results of simulations of stresses in the wall rock: (a) at the top of the tunnel, and (b) at the side of the tunnel, for a repository tunnel in fractured granite (thermal line load from a 37PWR-DPC emplaced at 100 or 150yOoR).

4.5 THM Response in Intact Granite with 37PWR DPCs

In the case of intact (unfractured) granite, we considered a case of rock characteristics somewhat similar to those at the Manitoba URL in Canada (Nguyen et al, 2009; Rutqvist et al., 2009b). Permeability and Young's modulus are set close to those of intact granite, i.e., k = 1×10^{-19} m^2 and E = 60 GPa. The value of

permeability is *in-between* that of argillite and fractured granite, whereas the Young's modulus is almost twice as high as that for fractured granite.

Simulations showed that both a significant thermal pressurization and thermal stress are taking place. The thermal pressurization causes a pressure increase that exceeds the lithostatic stress within 100 years (Figure 4-14b). The resulting peak of vertical tensile effective stress is about 7 MPa (Figure 4-15), while the horizontal effective compressive stress peaks at about 60 MPa. Such difference of stresses will likely induce shear activation of existing fractures and faults. The high rock thermal stresses may also cause significant stress changes at the tunnel wall with the compressive stress on top of the tunnel exceeding the spalling strength and a significant tensile stress at the side of the tunnel (Figure 4-16). Swelling stress within the buffer can prevent some of the spalling at the top of the tunnel, whereas the high tensile stress on the side of the tunnel could cause radial tensile fractures to develop.

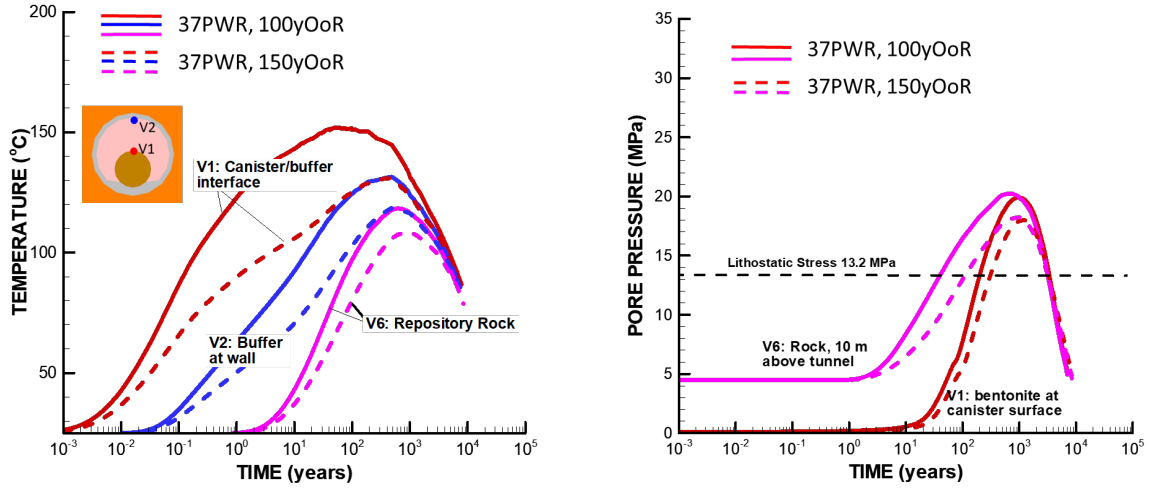

(a) (b)

Figure 4-14. Results of simulations of (a) temperature, and (b) pore pressure, demonstrating the impact of surface heat decay storage time (disposal at 100 or 150yOoR for a 37PWR DPC) on the thermal-hydraulic response for a repository tunnel in unfractured granite:

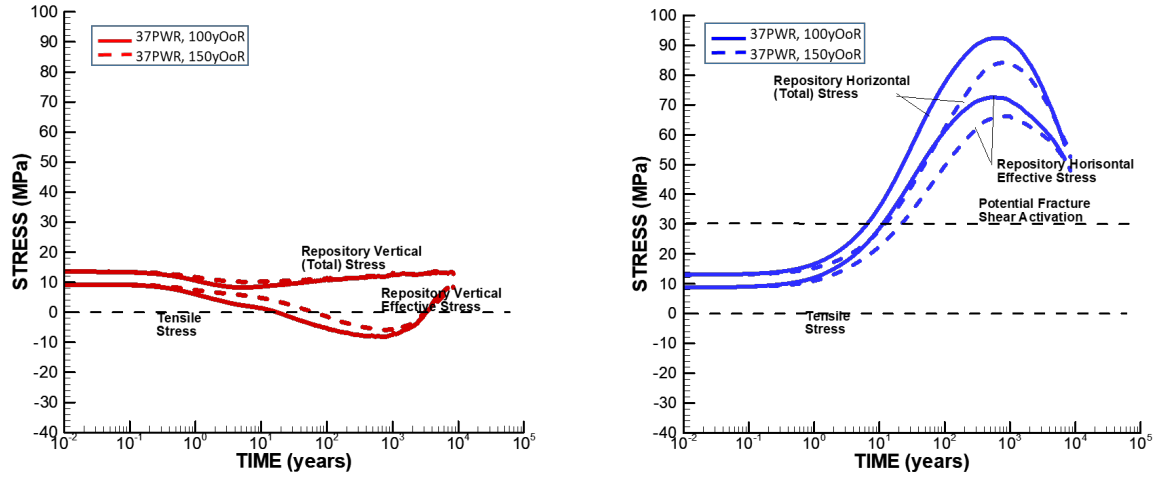

(a) (b)

Figure 4-15. Results of simulations of (a) vertical, and (b) horizontal stresses for a repository tunnel in unfractured granite (thermal line load from a 37PWR-DPC emplaced at 100 or 150yOoR).

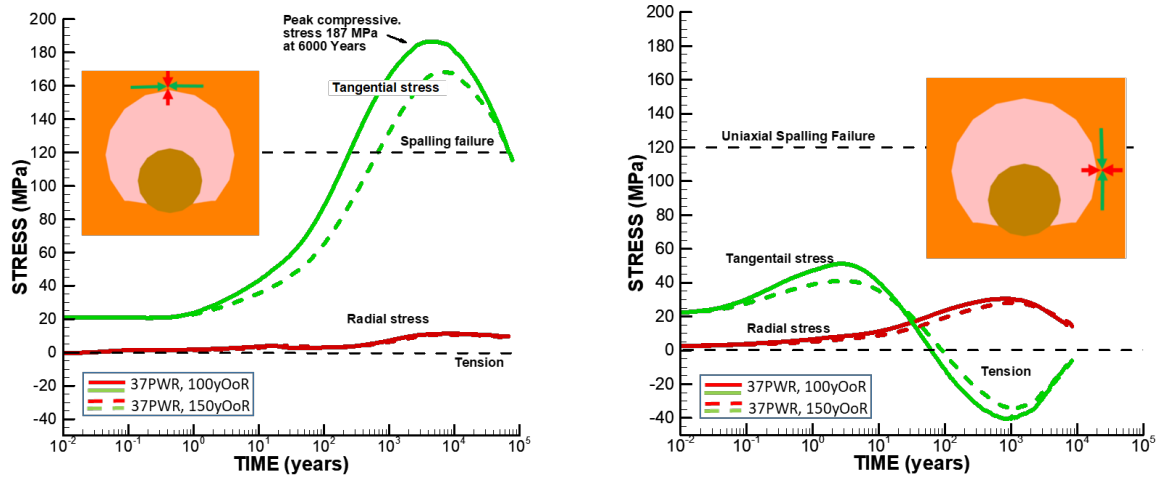

(a) (b)

Figure 4-16. Results of simulations of stresses in the wall rock: (a) at the top of the tunnel, and (b) at the side of the tunnel, for a repository tunnel in unfractured granite (thermal line load from a 37PWR-DPC emplaced at 100 or 150yOoR).

This page is intentionally left blank.

5. SUMMARY OF FY2019 PROGRESS AND FUTURE WORK

In FY2019, LBNL has initiated a new research activity addressing geotechnical and performance assessment of impacts of direct disposal of commercial spent nuclear fuel (SNF) in dual-purpose canisters (DPCs) in various host rock environments. The current work on modeling of DPSs and high-temperature impact builds upon previous SFWD work on modeling of coupled processes in argillite, crystalline and salt. Three-dimensional simulations are used for prediction of the detailed temperature evolution near the waste package, while two-dimensional simulations are employed for faster scoping simulations of various thermally induced coupled THM processes and geotechnical issues. Overall, the study highlights the importance of coupled THM processes for high-temperature systems, where damage could be caused around the waste emplacement tunnels and the host rock, if the systems are not properly designed. The following are some important findings from this study:

- The peak temperature in the buffer can be reduced if the buffer material is well designed. For example, by mixing the bentonite with graphite or graphene oxide, the buffer thermal conductivity can be significantly enhanced. The peak temperature will become close to the temperature of the host rock, reducing the thermal gradient across the buffer, thereby effectively eliminating drying of the bentonite near the waste canister. This might also be beneficial for timely resaturation and the development of a uniformly distributed swelling stress in the buffer.
- For a repository tunnel in argillite, the simulations show that thermal pressurization in host rock is of greatest concern as the fluid pressure could exceed the lithostatic stress, potentially inducing massive hydraulic fracturing. The thermal pressurization is driven by the temperature evolution in the host rock, which peaks about 1000 years after emplacement.
- For a repository tunnel in crystalline rock, fractured or intact granite, the thermal stress in the host rock is of greatest concern, as the induced horizontal thermal stress can cause shear activation of fractures in the host rock, and could cause compressive spalling failure and tensile failure in the tunnel wall. The thermal stresses peak several thousand years after emplacement, and could cause unwanted changes in permeability in the EDZ of emplacement tunnels and surrounding rock mass.

Thermal management in nuclear waste disposal is usually focusing on temperature evolution in the buffer and the near field zone. The study shows that more attention should the paid to the evaluation of the repository temperature away from the emplacement tunnel, as the repository temperature drives the stress changes and geomechanical changes around the emplacement tunnel. This is illustrated in Figure 5-1, showing that temperature in the buffer can be controlled to become close to that of the near field rock, whereas the far field temperature controls the thermal pressurization and the potential for hydraulic fracturing of the host rock. Moreover, high shear stresses and potential shear activation of existing fractures and faults may cause induced seismicity. This issue should be considered in the thermal management of a high-temperature nuclear waste disposal site.

For the rest of FY2019, the analysis will be expanded to the case of emplacement in alluvial, unsaturated sediments in line with current GDSA modeling at SNL. The material properties and conditions should be made consistent with those used in the current GDSA at SNL. Controls of the temperature evolution in the host rock through changes in the spacing between waste canisters and emplacement tunnels will be investigated. Moreover, analysis of direct disposal of DPCs in salt host rocks will be conducted; a rock type that might be most suitable for its high thermal conductivity and accelerated creep closure with temperature. On the other hand, the heavy canisters might sink because of creep deformations that are accelerated due to high temperature. These geotechnical issues will be further investigated to obtain the information needed for the design of direct disposal of DPCs in various host rocks.

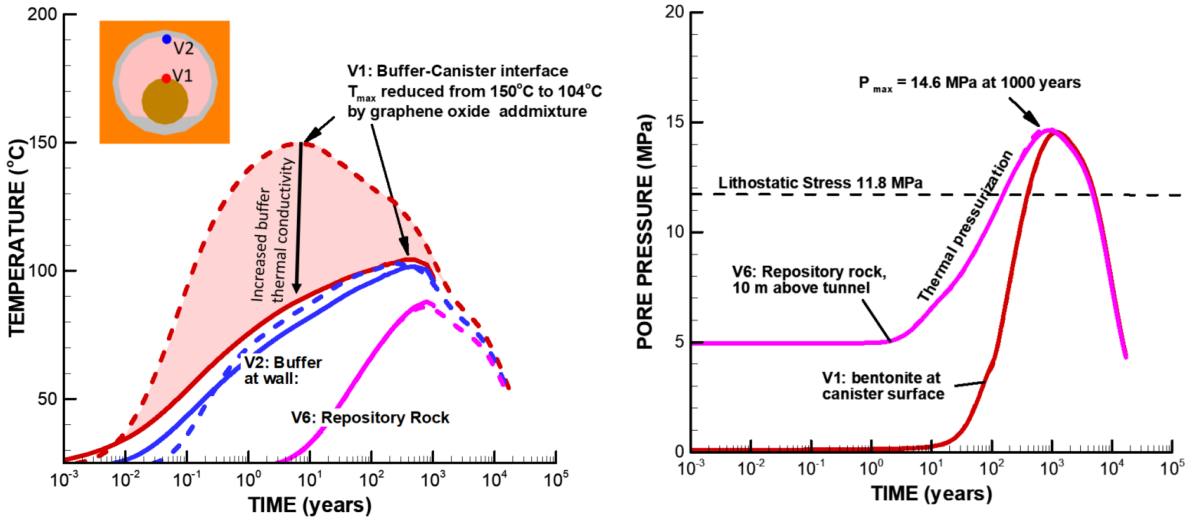

(a) (b)

Figure 5-1. Results of simulations of (a) temperature, and (b) pressure, showing the impact of engineered buffer material with enhanced thermal conductivity (heat source from a 24PWR-100yOoR DPC). Figure 5-1a shows a reduced peak temperature. Dashed lines are the results for the original unmodified bentonite thermal properties, and solid lines are the results for enhanced thermal conductivity. These results illustrate the fact that the thermal conductivity of the buffer impacts the temperature within the buffer itself, but have not significantly impacted THM responses in the surrounding rock.

6. ACKNOWLEDGEMENTS

This work was supported by the Spent Fuel and Waste Science and Technology Campaign, Office of Nuclear Energy, of the U.S. Department of Energy under Contract Number DE-AC02-05CH11231 with Lawrence Berkeley National Laboratory.

This page is intentionally left blank.

7. REFERENCES

Chen YG, Liu, X.M., Mu, X., Ye, W.M., Cui, Y.J., Chen, B., and Wu, D.B. (2018) Thermal conductivity of compacted GO-GMZ bentonite used as buffer material for a high-level Radioactive waste repository. Advances in Civil Engineering, 2018, Article ID 9530813, https://doi.org/10.1155/2018/9530813.

Hardin, E.L., Clayton, D.J., Howard, R.L., Scaglione, J.M., Pierce, E., Banerjee, K., Voegele, M.D., Greenberg, H.R., Wen, J., Buscheck, T.A., Carter, J.T., Severynse, T., and Nutt, W.M. (2013) Preliminary Report on Dual-Purpose Canister Disposal Alternatives (FY13). FCRD-UFD-2013-000171 Rev. 1. U.S. Department of Energy, Office of Used Nuclear Fuel Disposition.

Hardin, E, Bryan, C., Ilgen, A., Kalinina, E., Banerjee, K., Clarity, J., Howard, R., Jubin, R., Scaglione, J., Perry, F., Zheng, L., Rutqvist, J., Birkholzer, J., Greenberg, H., Carter, J., and Severynse, T. (2014) Investigations of Dual-Purpose Canister Direct Disposal Feasibility (FY14). FCRD-UFD-2014-000069 Rev. 0. U.S. Department of Energy, Office of Used Nuclear Fuel Disposition.

Hardin, E., Price, L., Kalinina, E., Hadgu, T., Ilgen, A., Bryan, C., Scaglione, J., Banerjee, K., Clarity, J., Jubin, R., Sobes, V., Howard, R., Carter, J., Severynse, T., Perry, F. (2015) Summary of Investigations on Technical Feasibility of Direct Disposal of Dual-Purpose Canisters. FCRD-UFD-2015-000129 Rev. 0. U.S. Department of Energy, Office of Used Nuclear Fuel Disposition.

Jobmann, M., and Buntebarth. G. (2009) Influence of graphite and quartz addition on the thermo–physical properties of bentonite for sealing heat-generating radioactive waste. Applied Clay Science 44, 206–210.

Nguyen, T.S., Börgesson, L., Chijimatsu, M., Hernelind, J., Jing, L., Kobayashi, A., and Rutqvist, J. (2009) A case study on the influence of THM coupling on the near field safety of a spent fuel repository in sparsely fractured granite. Environmental Geology, 57, 1239–1254.

Rutqvist, J., Bäckström, A., Chijimatsu, M., Feng, X.-T., Pan, P.-Z., Hudson, J., Jing, L., Kobayashi, A., Koyama, T., Lee, H.-S., Huang, X.-H., Rinne, M., and Shen, B. (2009a) Multiple-code simulation study of the long-term EDZ evolution of geological nuclear waste repositories. Environmental Geology, 57, 1313–1324.

Rutqvist, J., Börgesson, L., Chijimatsu, M., Hernelind, J., Jing, L., Kobayashi, A., and Nguyen S. (2009b) Modeling of damage, permeability changes and pressure responses during excavation of the TSX tunnel in granitic rock at URL, Canada. Environmental Geology, 57, 1263–1274.

Rutqvist, J., Barr, D., Birkholzer, J.T., Fujisaki, K., Kolditz, O., Liu, Q.-S., Fujita, T., Wang, W., and Zhang, C.-Y. (2009c) A comparative simulation study of coupled THM processes and their effect on fractured rock permeability around nuclear waste repositories. Environmental Geology, 57, 1347–1360.

Rutqvist, J., Ijiri, Y., and Yamamoto, H. (2011) Implementation of the Barcelona Basic Model into TOUGH-FLAC for simulations of the geomechanical behavior of unsaturated soils. Computers & Geosciences, 37, 751–762.

Rutqvist, J., Zheng, L., Chen, F., Liu, H.-H., and Birkholzer, J. (2014) Modeling of Coupled Thermo-Hydro-Mechanical Processes with Links to Geochemistry Associated with Bentonite-Backfilled Repository Tunnels in Clay Formations. Rock Mechanics and Rock Engineering, 47, 167–186.

Rutqvist, J., Kim, K., Xu, H., Guglielmi, Y., and Birkholzer, J. (2018) Investigation of Coupled Processes in Argillite Rock: FY18 Progress. Prepared for U.S. Department of Energy, Spent Fuel and Waste Disposition, LBNL-2001168, Lawrence Berkeley National Laboratory.

Rutqvist, J., Guglielmi, Y., Kim, K., Xu, H., Deng, H., Li, P., Hu, M., Steefel, C., Gilbert, B., Rinaldi, A., Nico, P., Borglin, S., Fox, P., and Birkholzer, J. (2019). Investigation of coupled processes in argillite rock: FY19 progress. Prepared for U.S. Department of Energy, Spent Fuel and Waste Disposition, LBNL-2001202, Lawrence Berkeley National Laboratory.